



HAL
open science

An Improved Ensemble Extreme Learning Machine Classifier for Detecting Diabetic Retinopathy in Fundus Images

R. Kalaiselvi, V. Desika Vinayaki

► **To cite this version:**

R. Kalaiselvi, V. Desika Vinayaki. An Improved Ensemble Extreme Learning Machine Classifier for Detecting Diabetic Retinopathy in Fundus Images. 5th International Conference on Computational Intelligence in Data Science (ICCIDS), Mar 2022, Virtual, India. pp.332-344, 10.1007/978-3-031-16364-7_26 . hal-04381280

HAL Id: hal-04381280

<https://inria.hal.science/hal-04381280v1>

Submitted on 9 Jan 2024

HAL is a multi-disciplinary open access archive for the deposit and dissemination of scientific research documents, whether they are published or not. The documents may come from teaching and research institutions in France or abroad, or from public or private research centers.

L'archive ouverte pluridisciplinaire **HAL**, est destinée au dépôt et à la diffusion de documents scientifiques de niveau recherche, publiés ou non, émanant des établissements d'enseignement et de recherche français ou étrangers, des laboratoires publics ou privés.



Distributed under a Creative Commons Attribution 4.0 International License



This document is the original author manuscript of a paper submitted to an IFIP conference proceedings or other IFIP publication by Springer Nature. As such, there may be some differences in the official published version of the paper. Such differences, if any, are usually due to reformatting during preparation for publication or minor corrections made by the author(s) during final proofreading of the publication manuscript.

An improved Ensemble Extreme Learning Machine classifier for detecting diabetic retinopathy in fundus images

V. Desika Vinayaki ^{1*}

Department of Computer science and engineering,

Noorul Islam Centre for Higher Education, Kumaracoil, India

**Email: vdesika.id@gmail.com*

Dr. R. Kalaiselvi ²

Department of Computer science and engineering,

Noorul Islam Centre for Higher Education, Kumaracoil, India.

Abstract:- This paper presents an automatic diabetes Retinopathy (DR) detection system using fundus images. The proposed automatic DR screening model saves the time of the ophthalmologist in disease diagnosis. In this approach, the segmentation is conducted using an improved watershed algorithm and Gray Level Co-occurrence Matrix (GLCM) is used for feature extraction. **An improved Ensemble Extreme Learning Machine (EELM) is used for classification and its weights are tuned using the Crystal Structure Algorithm (CRYSTAL) algorithm which also optimizes the loss function of the EELM classifier.** The experiments are conducted using two datasets namely DRIVE and MESSIDOR by comparing the proposed approach against different state-of-art techniques such as Support Vector Machine, VGG19, Ensemble classifier, and Synergic Deep Learning model. When compared to existing methodologies, the proposed approach has sensitivity, specificity, and accuracy scores of 97%, 97.3%, and 98%, respectively.

Keywords:- Fundus image, diabetic retinopathy, DRIVE, CRYSTAL algorithm, Improved watershed algorithm, and Ensemble Extreme Learning Machine

1 Introduction

DR [1] is a major cause of blindness that normally occurs in diabetic patients. Diabetes is caused by a high blood glucose level in the blood, which affects the patient's internal organs as well as their eyes. The different diseases caused in the eye by diabetes are

cataracts, glaucoma, and DR. The main reason for DR is the fluid leak in the small blood vessels which mainly results in visual loss. Based on the reports published by WHO, DR is the main reason for the 2.6% of deaths that occur worldwide. DR can also occur due to hereditary reasons. It is classified into three types namely: Proliferative, non-proliferative, and diabetic maculopathy. In this paper, we are mainly focusing on the non-proliferative DR known as exudates which are mostly known as hard exudates and various authors presented different techniques to identify the exudates in the retina [2].

Different vision-related issues arise when the tiny blood vessels in the retina are damaged. If early identification and treatment are not provided, the patient will lose all of his or her eyesight. In the earlier stages, this disease does not cause any symptoms and is only detected in different tests such as pupil dilation, visual acuity, etc [3]. To prevent vision loss in diabetic patients, early DR diagnosis is necessary. The existing systems are both processing intensive and consume higher time [4]. The ophthalmologists mainly identify DR via lesions and vascular abnormalities, even though this is highly effective it is resource-intensive in nature. Since the diabetes rate in the local population is high, experienced professionals and equipment are scarce in many areas. This arises the need for an automated DR detection system to prevent more people from blindness. This can be achieved via image processing, pattern recognition, and machine learning techniques invented which have been gained quite a high popularity [5].

The first issue is identifying a high-quality dataset with accurate labels [6,7]. Since there are more high-quality datasets available for the DR problem, several researchers face the challenge of unbalanced data. The next challenge is the problem associated with deep learning model design. The deep learning models are often prone to overfitting and underfitting issues and they also have to be trained via different trial and error methods. The main point to be noted here is the loss value obtained should be low and the learning capability should be high. The hyperparameter tuning process of the deep learning classifiers is another big issue that needs to be tackled. The limited processing resources, high time consumption, high false positives, and low accuracy is the problems faced by most of the existing techniques. To tackle these issues, in this paper we propose a Crystal Structure Algorithm (CRYSTAL) algorithm optimized Ensemble Extreme Learning Machine (EELM) architecture for DR classification. The major contributions of this paper are delineated as follows:

- This paper uses GLCM for feature extraction and an improved watershed algorithm for segmentation.
- The CRYSTAL optimized EELM classifier classifies the input obtained after segmentation and feature extraction into three types namely exudates, Micro Aneurysms, and Hemorrhages. The model proposed minimizes the time complexity and intricate processing issues associated with the state-of-art classifiers.

- The efficiency of this technique is evaluated using two datasets(DRIVE and MESSIDOR) in terms of accuracy, sensitivity, specificity, ROC curve, and confusion matrix.

The rest of this paper is arranged accordingly. Section 2 presents the related works and Section 3 elaborates the different steps incorporated in the proposed methodology in detail. Section 4 summarizes the findings of the proposed methodology acquired by testing the approach using two datasets in terms of different performance measures, and Section 5 concludes the paper.

2 Review of related works

The different works conducted by various authors in this domain are represented as follows: Saranya P et al. [8] utilized Convolutional Neural Network (CNN) for automatically identifying the non-proliferative diabetic retinopathy present in retinal fundus images. They evaluated their model on two popular datasets namely MESSIDOR and IDRiD. This work mainly reads the data from the image information and identifies the severity of DR. This technique has been mainly designed to be run in small and compact systems. This method offers a maximum accuracy of 90.89% in the MESSIDOR dataset.

Kanimozhi J et al.[9] presented an automatic lesion detection model for identifying the severity of DR via screening. Luminosity, contrast enhancement, blood vessel, and optic disc removal, and lesion detection and classification are the main steps. Contrast limited adaptive histogram equalization (CLAHE) and gamma correction are utilized for contrast and luminosity enhancement. Using morphological operations and classification, the lesions are identified after background removal. The efficiency of this technique is evaluated via the publicly available

Dutta A et al. [10] used individual retinal image features to identify the grades (binary or multiclass classification) of DR. They are identifying the different DR grades by integrating different machine learning classifiers by applying both single and multiple features observed. A fine-tuned VGG-19 model powered using transfer learning is used to evaluate the efficiency of this technique on both single and multiclass classifications of digital fundus images. The results show that the accuracy is improved up to 37% when compared to the existing models. This work helps the ophthalmologist to identify the different grades of DR from a single feature alone.

Melo T et al. [11] detected microaneurysm in color eye fundus images using a sliding band filter and ensemble classifier. The initial microaneurysm candidates are obtained via the sliding band filter technique and the final classification is done by a set of ensemble classifiers. Based on the confidence value assigned for each sample, a score is computed. This technique yields a sensitivity value of 64% and 81% for the e-ophta MA and SCREEN-DR dataset respectively. Pachiyappan A et al.[14] utilized morphological operators for identifying the DR from fundus images. The model was trained using 85

fundus images where at least 85 images have a presence of mild retinopathy. The accuracy of this technique is estimated to be 97.75% for optical disk detection.

Shankar K et al. [12] utilized a Synergic Deep Learning (SDL) model for detecting DR from the fundus images. Their model mainly classifies the RD cases based on their severity. The different stages involved in the proposed work are pre-processing, segmentation, and classification. In the preprocessing stage, the unnecessary noises are removed such as the edges in the images, and the region of interest is extracted using the histogram-based segmentation technique. The SDL model classifies the output based on the different levels of severity using the Messidor DR dataset. However, the authors have not taken steps to overcome the complexity associated with the SDL model.

Katada Y et al.[13] utilized artificial intelligence techniques for automatically screening the DR from fundus images. They utilized both Japanese and American datasets for these experiments and classified the input images based on the severity level. A Deep Convolutional Neural Network (DCNN) and Support Vector Machine (SVM) classifier are trained using the 35,1256 and 200 fundus images acquired from both the American and Japanese datasets. For the Japanese dataset, their model provided a sensitivity and specificity score of 81.5% and 71.9% respectively. For the American dataset, their model yielded a sensitivity and specificity score of 81.5% and 71.9%.

3 Proposed Methodology

In this work, we mainly aim to classify the DR fundus images with a maximum detection rate. The overall architecture of the proposed work is depicted in Figure-1. The steps used in the proposed work are presented as follows:

3.1 Image preprocessing:

Initially, the input image from the DRIVE and MESSIDOR dataset is preprocessed using the adaptive histogram equalization technique, image enhancement and resizing techniques [18]. In this step, the background is normalized and illumination is equalized.

3.2 Image segmentation:

The segmentation process is mainly applied to the optical disk region of the fundus image. The optical disk is the brightest part in the fundus image and is based on the intensity value it is extracted. The segmentation process is mainly conducted using the improved watershed algorithm [17]. The reason for selecting this algorithm is its capability to identify the bright areas and solve the low color discrimination problem. In this way, this algorithm helps in improving the accuracy of the classifier even more. The threshold value is mainly selected by the assumption that it should not exceed the maximum intensity value of the fundus image. The region in the optical disk is identified

by segmenting the region around the final optimal disk candidate. The boundary of the optical disk can be identified via the thresholded region.

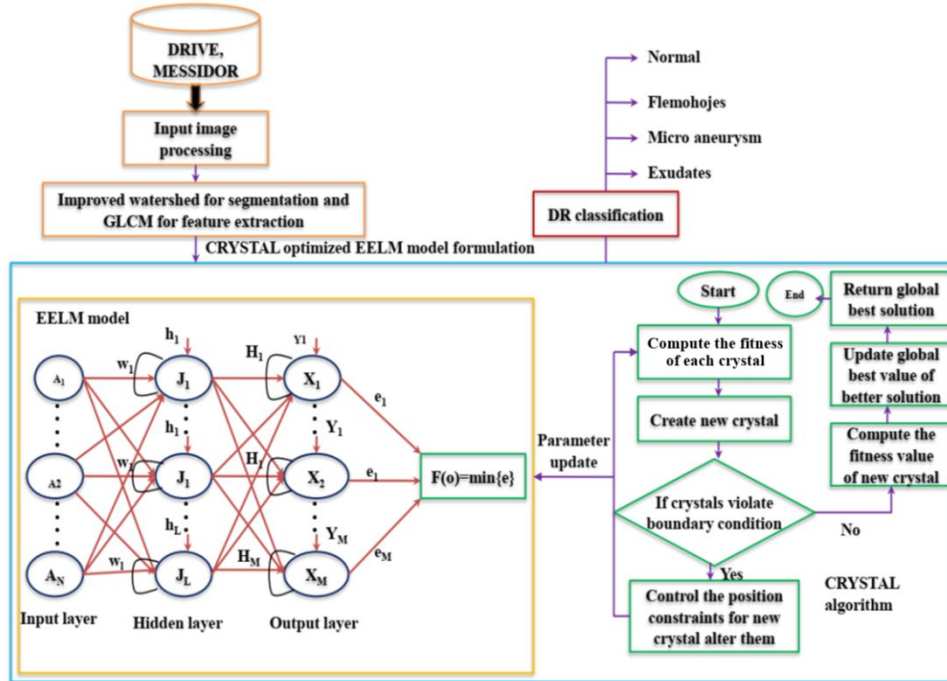


Figure-1: Proposed architecture

3.3 Feature extraction using GLCM:

The preprocessed image is given as an input to the GLCM [16] for retina removal and blood vessel segmentation. The GLCM is mainly applied to the preprocessed image. The heterogeneous surfaces can be identified via the GLCM indices and the texture is the term used in GLCM to identify the grey level variations and tones present in the input fundus image. Every GLCM index highlights a certain property such as irregularity, smoothness, etc. The GLCM structure is formulated as follows: Initially, a grayscale matrix of the image is transformed into an integer matrix by dividing the continuous pixel value range to M bins. The bins are equally valued and are mapped into a single grey level. The pixel adjacency can be represented using four different angles: 0° , 45° , 90° , and 135° . The generic element of the matrix is represented as $g(x,y)$. The details of the GLCM indices selected are presented in Table-1.

Table-1: GLCM indices description

Name	Description
Contrast	The change in the grey level pixels present in between continuous pixels is noted and exponential weightage is given.
Homogeneity	The similarity of the grey level pixels to their neighboring pixels is measured
Dissimilarity	The elements are weighted linearly.
Entropy	The disorder of the image is measured here which is negatively interrelated with the energy.
Energy	The pixel pair repetition and texture uniformity are measured here. A constant grey level distribution possesses a high energy value.
Mean	The average value of the grey level pixels in the image is computed
Variance	When there is a variation of the grey level values when compared to the mean, variance increases which is mainly a measure of homogeneity
Correlation	The linear dependency of the image is measured in relation to the adjacent and grey level pixels

3.4 CRYSTAL optimized EELM classifier

GS algorithm: The crystalline solids structure is the basic concept of crystal structure (CS) algorithm [15]. Various geometrical structures is defined as the Lattice and the Bravais model (A) describes the mathematical representation of lattice.

$$A = \sum m_i B_i \quad (1)$$

where m_i is the integer and B_i represent the smallest path with respect to the directions of principal crystallographic. From this, i denote the number of corners in the crystals.

Mathematical model: In the lattice space, the single crystal deems optimized candidate solutions. For the iterative purposes, determines the number of crystals.

$$D = \begin{bmatrix} D_1 \\ D_2 \\ \vdots \\ D_3 \\ \vdots \\ D_n \end{bmatrix} = \begin{bmatrix} z_1^1 & z_1^2 & \dots & z_i^j & \dots & z_1^d \\ z_2^1 & z_2^2 & \dots & z_2^1 & \dots & z_2^d \\ \vdots & \vdots & \vdots & \vdots & \vdots & \vdots \\ z_i^1 & z_i^2 & \dots & z_i^j & \dots & z_i^d \\ \vdots & \vdots & \vdots & \vdots & \vdots & \vdots \\ z_n^1 & z_n^2 & \dots & z_n^j & \dots & z_n^d \end{bmatrix}, \quad \begin{cases} i = 1, 2, \dots, m \\ j = 1, 2, \dots, c \end{cases} \quad (2)$$

where c describes the problem of dimensionality and m is the total number of crystals. In the search space of the network, the nodes are placed randomly.

$$z_i^j(0) = z_{i,\min}^j + \text{Random}(z_{i,\max}^j - z_{i,\min}^j) \quad (3)$$

From the above equation, $z_i^j(0)$ is the nodes initial population as well as $z_{i,\min}^j$ and $z_{i,\max}^j(0)$ are the minimal and maximal values. For the i^{th} candidate solution, the j^{th} decision variable with the random number tends to the interval $[0, 1]$.

The base nodes B_N and the best configuration with the randomly selected mean values and the best node configuration is M_D and D_O . The below-mentioned step describes the best candidate node from the network search space.

(a) **Cubicle based on best crystals:**

$$D_{new} = D_{old} + A_1 B_N + A_2 D_O \quad (4)$$

(b) **Simple Cubicle:**

$$D_{new} = D_{old} + A B_N \quad (5)$$

(c) **Cubicle depends on best and mean nodes:**

$$D_{new} = D_{old} + A_1 B_N + A_2 M_D + A_3 D_O \quad (6)$$

(d) **Cubicle based on mean nodes:**

$$D_{new} = D_{old} + A_1 B_N + A_2 M_D \quad (7)$$

From this, D_{new} and D_{old} describes the new and old updated positions, where, A_1 , A_2 , and A_3 are the random numbers.

3.5. EELM for classification

EELM is the modified version of the Single-layer Feed Forward Neural Network (SLFNN) [20]. The SLFNN comprises two different layers namely the input layer and the output layer. No computation is performed in the input layer and the output layer is obtained when diverse weights are applied on the input node. The EELM classifier is trained with the appropriate input images from the dataset to obtain the optimal outcome for the input. The reason the EELM architecture is selected in this work is for its improved generalization performance, faster learning speed, minimal training error, easier implementation, independence of user input data, and offers significant accuracy.

The GLCM features extracted is represented as M with an already specified target (A_i, Y_i) where $A_i = [A_{i1}, A_{i2}, \dots, A_{iM}]^T \in R^m$ and $Y_i = [Y_{i1}, Y_{i2}, \dots, Y_{iM}]^T \in R^n$. The total number of output classes is represented as m which is 4 in our paper. Each hidden node (H) in the

SLFNN network comprises of bias(β_i) and random weights(ω_i). Using the output weight matrix O_i and activation function Z , the output (X_i) of the SLNN is obtained and this process is explained as follows:

$$\sum_{k=1}^H O_i Z(\omega_i, \beta_i, A_i) = X_i; k = 1, 2, \dots, M \quad (8)$$

The zero mean error of the $\sum_{k=1}^H O_i Z(\omega_i, \beta_i, A_i) = \|X_i - Y_i\|; k = 1, 2, \dots, M$ value is approximated using ω_i, β_i , and O_i and it is represented as follows:

$$\sum_{k=1}^H O_i Z(\omega_i, \beta_i, A_i) = Y_i; k = 1, 2, \dots, M \quad (9)$$

The above M equations can be compressed using a hidden layer output matrix (J) as follows:

$$JO = Y \quad (10)$$

By utilizing the smallest norm least square equation, the output weight matrix \hat{O} is computed as follows:

$$\hat{O} = J^+ Y \quad (11)$$

The J^+ value in the above equation mainly represents the Moore Penrose generalized inverse of J. The orthogonal projection technique is applied to prevent the singularity of the matrixes and the output weight matrix derived is presented as follows:

$$\hat{O} = \begin{cases} J^T \left(\frac{1}{\lambda} + JJ^T \right)^{-1} Y & ; \text{If } M < O \\ \left(\frac{1}{\lambda} + JJ^T \right)^{-1} YJ^T & ; \text{If } M > O \end{cases} \quad (12)$$

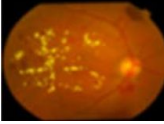
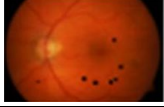
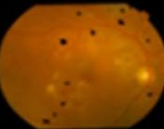
For each image sample, the input feature (A_i) is trained repeatedly to obtain the \hat{O} value of the EELM classifier. The weight assigned to each member of the ensemble is optimized using the CRYSTAL algorithm and the efficiency of the CRYSTAL algorithm is evaluated using the loss function. The predicted samples of root mean square error (RMSE) is the selected loss function. The below equation explains the RMSE value.

$$RMSE = \sqrt{\frac{1}{E} \sum_{g=1}^G \left(\hat{Z}_g - Z_g \right)^2} \quad (13)$$

The predicted model to the input is \hat{Z}_g and the real value is Z_g . The total amount of forecasted samples is G.

The proposed model classified three types of DR abnormalities namely Hemorrhages, Micro Aneurysms, and Exudates. The micro aneurysms are the initial stage of DR where red spots start appearing in the retina with a size of fewer than 125 μm . The lesions have sharp margins and mainly occur due to the weakness of the vessel walls. The hemorrhages have an irregular margin and are large in size ($>125 \mu\text{m}$). There are two types of exudates namely hard and soft. The hard exudates are mainly caused due to the leakage of plasma and they are in the form of bright yellow spots. The soft exudates are mainly caused due to the swelling in the nerve fiber and they are usually represented as visual spots. The three types of abnormalities classified by the proposed methodology are demonstrated in Table-2 and it is explained as follows:

Table-2: Classifications of DR abnormalities

Image	Corresponding classes
	Exudates
	Micro Aneurysms
	Hemorrhages

4 Experimental Results and Analysis

The proposed model is implemented in Matlab in a DELL Inspiron One 27 Ryzen 7 PC equipped with a 16 GB DDR4 RAM, 1 TB HD capacity, 256 GB SSD, and Windows 10 OS. The details of the dataset, performance metrics used, and the results observed are presented in this section.

4.1 Dataset description

Digital Retinal Images for Vessel Extraction dataset (DRIVE): The DRIVE [19] is a retina vessel segmentation dataset that comprises a total of 40 JPEG images. A total of 7 abnormal cases is found in this dataset. The image has a resolution of 584*565 pixels with eight bits per three color channel. The 40 images are partitioned in a 5:5 ratio where 20 images are used for testing and the remaining 20 are used for training.

Messidor dataset: This dataset comprises a total of 1200 eye fundus color images from which 800 images are obtained with pupil dilation and another 800 are obtained without pupil dilation [8]. The 1200 images in the dataset are partitioned into three sets which are then compressed into four subsets. In our proposed work, we partition this dataset in an 8: 2 ratio, where 80% of images are used for training while the remaining 20% is used for testing. The retinopathy grade is mainly given based on the number of microaneurysms, hemorrhages, and neovascularization.

4.2 Performance evaluation metrics

The different performance evaluation metrics used in this paper is presented as follows:

Sensitivity: It is the capability that the classifier can recognize the DR abnormalities correctly and it is computed as follows:

$$Sensitivity = \frac{A^+}{A^+ + B^-} \quad (15)$$

Specificity: The ability of the classifier to accurately reject the DR abnormalities correctly and it is computed as follows:

$$Specificity = \frac{A^-}{A^- + B^+} \quad (16)$$

Accuracy: It determines the capability of the classifier to accurately discriminate between the actual and predicted samples and it is computed as follows:

$$Accuracy = \frac{A^+ + A^-}{A^+ + A^- + B^+ + B^-} \quad (17)$$

Here the true positive, true negative, false positive, and false negative values are represented as A+, A-, B+, and B-.

ROC curve: The ROC curve plots two parameters namely the True positive rate and false positive rate and identifies the performance of the classifier at varying thresholds.

Confusion matrix: This matrix mainly identifies the confusion of the classifier in predicting two classes. It is mainly computed by evaluating the model on the testing data whose ground-truth value is actually known.

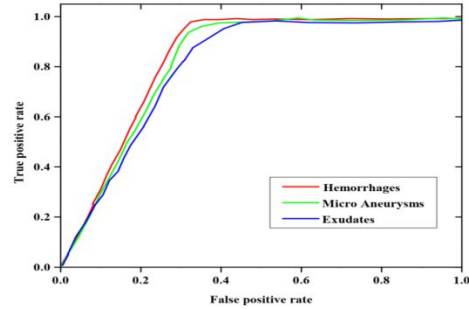


Figure-2: ROC classification results for three classes

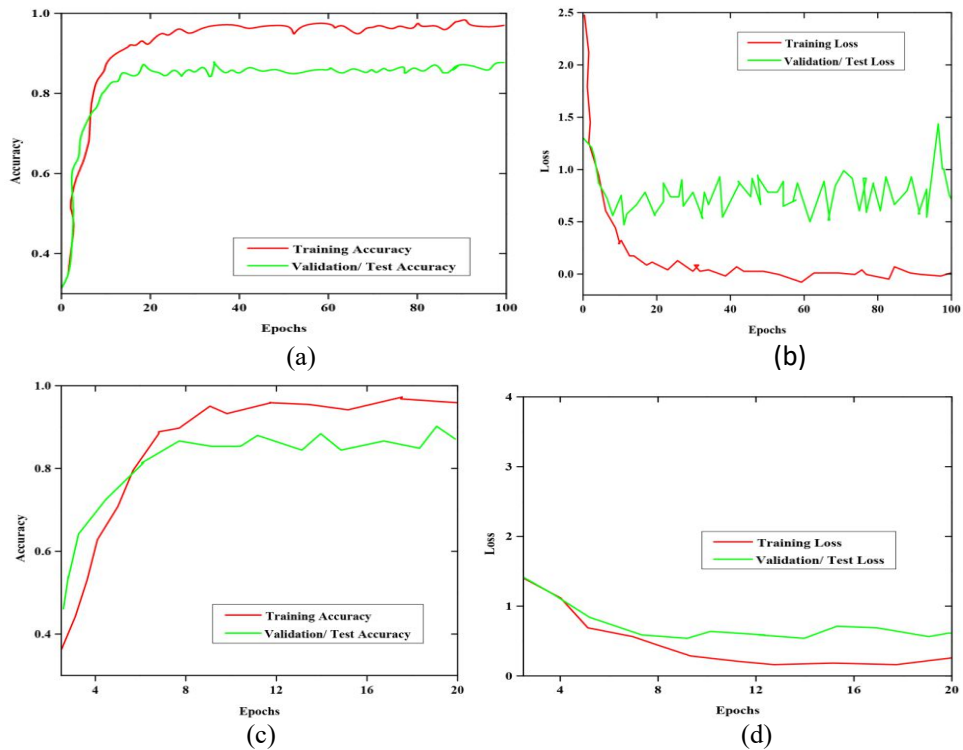


Figure-3: (a) Training and testing accuracy of DRIVE dataset (b) Training and testing loss of DRIVE dataset, (c) Training and testing accuracy of MESSIDOR dataset (d) Training and testing loss of MESSIDOR dataset

4.3 Results and discussion

The ROC curve obtained for the three classes is presented in Figure-2. The ROC curve shows improved classification accuracy for the three classes. The accuracy and the loss

curves of the proposed model on the two datasets (DRIVE and MESSIDOR) are presented in Figure-3 (a)- (d). For both the training and testing datasets, we can notice an exponential rise in the accuracy with an increase in the number of epochs. The loss percentage also decreases with an increase in the number of epochs. These results show the capability of the model in predicting the false positives and false negatives accurately.

The efficiency of the proposed model is evaluated using different performance metrics such as accuracy, sensitivity, specificity, and computational time. The results obtained are shown in Table-3 and it is self-explanatory. The proposed methodology takes a total of 15.36 seconds to identify the abnormalities present in the input dataset. The time efficiency of the proposed model shows its efficiency in reducing the ophthalmologist time for disease diagnosis. The efficiency of the proposed methodology is also compared with existing techniques such as CNN[8], VGG19[10], Ensemble [11], SDL [12], and SVM [13]. The experimental results demonstrate the proposed model's capability in identifying the DR accurately. Even though the deep learning models offer higher performance in terms of accuracy, sensitivity, and specificity, the time and computational complexity associated with it are high. The existing methodology mainly takes more time to diagnose due to the usage of intricate feature extraction techniques which individually take 10 minutes for processing. The segmentation and the feature extraction techniques used in our paper are also less time-consuming when compared to the existing techniques.

Table-3: Comparative analysis

Techniques	Sensitivity (%)	Specificity (%)	Accuracy	Computational time (seconds)
CNN[8]	91	91	91	85.36
VGG19 [10]	93	91	92	47.65
Ensemble [11]	87	85	84	19.36
SDL [12]	88	89	90	25.69
SVM [13]	86	85	84	17.56
Proposed method	97	97.3	98	15.36

Fig 4 expresses the results of the confusion matrix and the figure is plotted between the actual and predicted classes of diabetic retinopathy detections namely Hemorrhages, Micro Aneurysms, Exudates, and Normal classes. The accuracy value of each class is represented using green color.

Table 4 delineates the performance of the proposed model with respect to four different classes namely Hemorrhages, Micro Aneurysms, Exudates, and Normal classes. The accuracy, specificity, and sensitivity measures analyze the performance of these diabetic retinopathy classes. The accuracy, specificity, and sensitivity for Hemorrhages are 98.36%, 96.34%, and 95.56% as well as for Micro Aneurysms are 98.24%, 98.43%, and 96.34%. Based on the Exudates, we have obtained 98.42% accuracy, 94.47% specificity,

and 97.03% sensitivity results. For normal classes, the proposed method offered 98.31%, 97.78%, and 98.45% performance values are achieved with respect to the accuracy, specificity, and sensitivity results.

Actual class	Predicted class			
	Hemorrhages	Micro Aneurysms	Exudates	Normal
Hemorrhages	98.36%	1.25%	0.39%	0%
Micro Aneurysms	0%	98.24%	0.78%	0.98%
Exudates	0.96%	0%	98.42%	0.62%
Normal	0.67%	1.02%	0%	98.31%

Figure 4: Confusion matrix

Table 4: Performance analysis of proposed method based on different classes

Name of the classes	Performance metrics		
	<i>Accuracy</i>	<i>Specificity</i>	<i>Sensitivity</i>
<i>Hemorrhages</i>	98.36%	96.34%	95.56%
<i>Micro Aneurysms</i>	98.24%	98.43%	96.34%
<i>Exudates</i>	98.42%	94.47%	97.03%
<i>Normal</i>	98.31%	97.78%	98.45%

5 Conclusion

This paper presents an efficient DR diagnosis system that improves the decision-making capability of ophthalmologists. A CRYSTAL optimized EELM architecture is proposed in this paper to identify the three different types of DR classes namely exudates, Micro Aneurysms, and Hemorrhages. The efficiency of this methodology is verified using two different datasets namely DRIVE and MESSIDOR. The GLCM technique is used for feature extraction and the improved watershed algorithm is used for segmentation. The CRYSTAL optimized EELM architecture is used for classification. The efficiency of the proposed technique is evaluated in terms of sensitivity, specificity, ROC curve, and confusion matrices. The proposed approach offers sensitivity, specificity, and accuracy score of 97%, 97.3%, and 98% when compared to the existing techniques. The computational time of the proposed methodology is 15.36 seconds which is relatively low than the other techniques. In the future, we plan to identify the different types of glaucoma in diabetic patients.

References:

1. Kadan, A.B. and Subbian, P.S., 2021. Diabetic Retinopathy Detection from Fundus Images Using Machine Learning Techniques: A Review. *Wireless Personal Communications*, 121(3), pp.2199-2212.
2. Akram, M.U., Akbar, S., Hassan, T., Khawaja, S.G., Yasin, U. and Basit, I., 2020. Data on fundus images for vessels segmentation, detection of hypertensive retinopathy, diabetic retinopathy and papilledema. *Data in brief*, 29, p.105282.
3. Tsiknakis, N., Theodoropoulos, D., Manikis, G., Ktistakis, E., Boutsora, O., Berto, A., Scarpa, F., Scarpa, A., Fotiadis, D.I. and Marias, K., 2021. Deep learning for diabetic retinopathy detection and classification based on fundus images: A review. *Computers in Biology and Medicine*, 135, p.104599.
4. Ravishankar, S., Jain, A. and Mittal, A., 2009, June. Automated feature extraction for early detection of diabetic retinopathy in fundus images. In *2009 IEEE Conference on Computer Vision and Pattern Recognition* (pp. 210-217). IEEE.
5. Bonaccorso, G., 2018. *Machine Learning Algorithms: Popular algorithms for data science and machine learning*. Packt Publishing Ltd.
6. Dai, L., Fang, R., Li, H., Hou, X., Sheng, B., Wu, Q. and Jia, W., 2018. Clinical report guided retinal microaneurysm detection with multi-sieving deep learning. *IEEE transactions on medical imaging*, 37(5), pp.1149-1161.
7. Fu, H., Wang, B., Shen, J., Cui, S., Xu, Y., Liu, J. and Shao, L., 2019, October. Evaluation of retinal image quality assessment networks in different color-spaces. In *International Conference on Medical Image Computing and Computer-Assisted Intervention* (pp. 48-56). Springer, Cham.
8. Saranya, P. and Prabakaran, S., 2020. Automatic detection of non-proliferative diabetic retinopathy in retinal fundus images using convolution neural network. *Journal of Ambient Intelligence and Humanized Computing*, pp.1-10.
9. Kanimozhi, J., Vasuki, P. and Roomi, S.M.M., 2020. Fundus image lesion detection algorithm for diabetic retinopathy screening. *Journal of Ambient Intelligence and Humanized Computing*, pp.1-10.
10. Dutta, A., Agarwal, P., Mittal, A. and Khandelwal, S., 2021. Detecting grades of diabetic retinopathy by extraction of retinal lesions using digital fundus images. *Research on Biomedical Engineering*, 37(4), pp.641-656.
11. Melo, T., Mendonça, A.M. and Campilho, A., 2020. Microaneurysm detection in color eye fundus images for diabetic retinopathy screening. *Computers in Biology and Medicine*, 126, p.103995.
12. Shankar, K., Sait, A.R.W., Gupta, D., Lakshmanaprabu, S.K., Khanna, A. and Pandey, H.M., 2020. Automated detection and classification of fundus diabetic retinopathy images using synergic deep learning model. *Pattern Recognition Letters*, 133, pp.210-216.

13. Katada, Y., Ozawa, N., Masayoshi, K., Ofuji, Y., Tsubota, K. and Kurihara, T., 2020. Automatic screening for diabetic retinopathy in interracial fundus images using artificial intelligence. *Intelligence-Based Medicine*, 3, p.100024.
14. Pachiyappan, A., Das, U.N., Murthy, T.V. and Tatavarti, R., 2012. Automated diagnosis of diabetic retinopathy and glaucoma using fundus and OCT images. *Lipids in health and disease*, 11(1), pp.1-10.
15. Talatahari, S., Azizi, M., Tolouei, M., Talatahari, B. and Sareh, P., 2021. Crystal Structure Algorithm (CryStAl): A Metaheuristic Optimization Method. *IEEE Access*, 9, pp.71244-71261.
16. Park, Y. and Guldmann, J.M., 2020. Measuring continuous landscape patterns with Gray-Level Co-Occurrence Matrix (GLCM) indices: An alternative to patch metrics?. *Ecological Indicators*, 109, p.105802.
17. Zhang, L., Zou, L., Wu, C., Jia, J. and Chen, J., 2021. Method of famous tea sprout identification and segmentation based on improved watershed algorithm. *Computers and Electronics in Agriculture*, 184, p.106108.
18. Dubey, V. and Katarya, R., 2021, May. Adaptive Histogram Equalization based Approach for SAR Image Enhancement: A Comparative analysis. In *2021 5th International Conference on Intelligent Computing and Control Systems (ICICCS)* (pp. 878-883). IEEE.
19. Niemeijer, J.S., Ginneken, B., Loog, M. and Abramoff, M., 2007. Digital retinal images for vessel extraction.
20. Sahani, M., Swain, B.K. and Dash, P.K., 2021. FPGA-based favourite skin colour restoration using improved histogram equalization with variable enhancement degree and ensemble extreme learning machine. *IET Image Processing*.